AD-A038 421 ARMY MISSILE RESEARCH DEVELOPMENT AND ENGINEERING LAB--ETC F/G 16/1
MECHANICAL BEHAVIOR OF FILAMENT-WOUND COMPOSITE TUBES.(U)
JAN 77 G A WEMPNER

UNCLASSIFIED RL-77-8 NL

1 OF 1
AD
A038421

END
DATE
FILMED
5-77

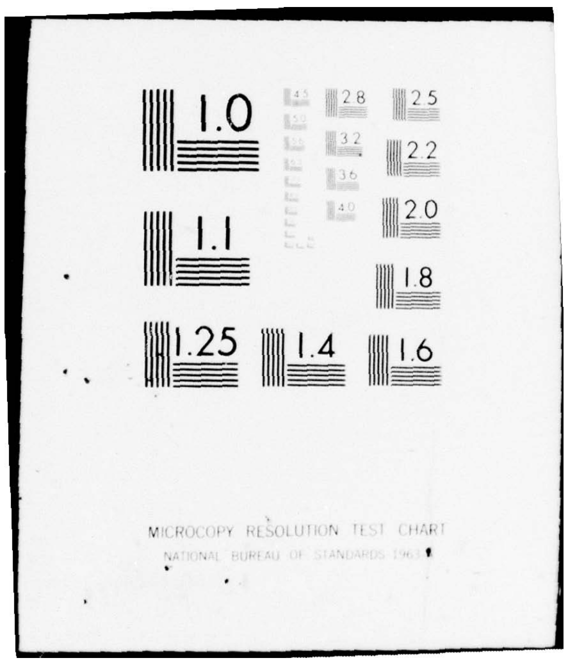
1.0
1.1
1.25
1.4
1.6
1.8
2.0
2.2
2.5
2.8
3.2
3.6
4.0
4.5
MICROCOPY RESOLUTION TEST CHART
NATIONAL BUREAU OF STANDARDS 1963 A

TECHNICAL REPORT RL-77-8

MECHANICAL BEHAVIOR OF FILAMENT–WOUND COMPOSITE TUBES

School of Engineering Science and Mechanics
Georgia Institute of Technology
Atlanta, Georgia 30332

14 January 1977

Approved for public release; distribution unlimited.

U.S. ARMY MISSILE COMMAND

Redstone Arsenal, Alabama

Prepared for

Ground Equipment and Materials Directorate
US Army Missile Research, Development and Engineering Laboratory
US Army Missile Command
Redstone Arsenal, Alabama 35809

FORM AMSMI-1021, 1 DEC 65 PREVIOUS EDITION IS OBSOLETE

DISPOSITION INSTRUCTIONS

DESTROY THIS REPORT WHEN IT IS NO LONGER NEEDED. DO NOT RETURN IT TO THE ORIGINATOR.

DISCLAIMER

THE FINDINGS IN THIS REPORT ARE NOT TO BE CONSTRUED AS AN OFFICIAL DEPARTMENT OF THE ARMY POSITION UNLESS SO DESIGNATED BY OTHER AUTHORIZED DOCUMENTS.

TRADE NAMES

USE OF TRADE NAMES OR MANUFACTURERS IN THIS REPORT DOES NOT CONSTITUTE AN OFFICIAL INDORSEMENT OR APPROVAL OF THE USE OF SUCH COMMERCIAL HARDWARE OR SOFTWARE.

UNCLASSIFIED

SECURITY CLASSIFICATION OF THIS PAGE (When Data Entered)

REPORT DOCUMENTATION PAGE

READ INSTRUCTIONS BEFORE COMPLETING FORM

1. REPORT NUMBER 14
RL-77-8

2. GOVT ACCESSION NO.

3. RECIPIENT'S CATALOG NUMBER

4. TITLE (and Subtitle) 6
MECHANICAL BEHAVIOR OF FILAMENT-WOUND COMPOSITE TUBES,

5. TYPE OF REPORT & PERIOD COVERED 9
Technical Report,

6. PERFORMING ORG. REPORT NUMBER
RL-77-8

7. AUTHOR(s) 10
G. A. Wempner

8. CONTRACT OR GRANT NUMBER(s)
16

9. PERFORMING ORGANIZATION NAME AND ADDRESS
School of Engineering Science and Mechanics
Georgia Institute of Technology
Atlanta, Georgia 30332

10. PROGRAM ELEMENT, PROJECT, TASK AREA & WORK UNIT NUMBERS
(DA) 1M362303A214
AMCMS Code 632303.11.21409

11. CONTROLLING OFFICE NAME AND ADDRESS
Commander
US Army Missile Command
Attn: DRSMI-RPR
Redstone Arsenal, Alabama 35809

12. REPORT DATE 11
14 January 1977

13. NUMBER OF PAGES
17

14. MONITORING AGENCY NAME & ADDRESS (if different from Controlling Office)
Commander
US Army Missile Command
Attn: DRSMI-RL
Redstone Arsenal, Alabama 35809

12 17p.

15. SECURITY CLASS. (of this report)
Unclassified

15a. DECLASSIFICATION/DOWNGRADING SCHEDULE

16. DISTRIBUTION STATEMENT (of this Report)

Approved for public release; distribution unlimited.

17. DISTRIBUTION STATEMENT (of the abstract entered in Block 20, if different from Report)

18. SUPPLEMENTARY NOTES

19. KEY WORDS (Continue on reverse side if necessary and identify by block number)

Filament-wound tube
Modes of failure
Internal pressure

20. ABSTRACT (Continue on reverse side if necessary and identify by block number)

The main component of a lightweight missile launcher is a cylindrical tube which is formed by a helical winding of glass filaments embedded in epoxy resin. In service, the tube is subjected to extreme internal pressure. Consequently, knowledge concerning the mechanisms of failure under pressure is vital to the analysis and design of these tubes. This report identifies the mechanisms of failure and offers appropriate methods to compute the ultimate pressure.

DD FORM 1 JAN 73 1473 EDITION OF 1 NOV 65 IS OBSOLETE

UNCLASSIFIED

SECURITY CLASSIFICATION OF THIS PAGE (When Data Entered)

400 406

ACCESSION for

NTIS White Section ☑

DDC Buff Section ☐

UNANNOUNCED ☐

JUSTIFICATION ....

....

BY ....

DISTRIBUTION/AVAILABILITY CODES

Dist.	AVAIL. and/or SPECIAL	
A		

CONTENTS

ACKNOWLEDGMENTS

The work presented in this report was sponsored by the US Army Missile Command, Ground Equipment and Materials Directorate, under Scientific Services Agreement DAAG29-76-D-0100 with Battelle Columbus Laboratories and was administered by the Scientific Services Program.

The author is indebted to: Mr. Glen Clodfelter for his valuable insights and excellent data, Mr. Richard Thompson for numerous helpful suggestions, Mr. Grady Patrick for his computational assistance, and Mr. Will Lewis for his support and encouragement.

I. INTRODUCTION

The main component of a lightweight missile launcher is a cylindrical tube which is formed by a helical winding of glass filaments embedded in epoxy resin. In service, the tube is subjected to extreme internal pressure. Consequently, knowledge concerning the mechanisms of failure under pressure is vital to the analysis and design of these tubes. The extensive tests performed by Clodfelter[1] provide valuable data and insights which reveal various modes-of-failure and indicate alternative methods of analysis.

This report identifies the mechanisms of failure and offers appropriate methods to compute the ultimate pressure.

II. MODES OF FAILURE

Three distinct modes-of-failure are observed:

a) Tearing — A form of rupture which is initiated by crazing and/or debonding which causes leakage. Such tearing may be caused by membrane or bending actions.

b) Bursting — An abrupt rupture at the ultimate strength of the filaments. Crazing and debonding occurs prior to bursting.

c) Buckling — Initiates overall bending and precipitates rupture.

Each mode-of-rupture is associated with a distinct mechanism and is intimately related to the angle of wrapping. Tearing depends upon the strength of the resin and the bond. Bursting depends largely upon the strength of the filaments. Buckling is mainly dependent upon the stiffness of the composite. A description of each mechanism is presented in the following paragraphs.

A. Tearing

Tearing occurs if the resin and/or bond fails (crazing and/or debonding), and if the state of strain tends to dilate the composite, therefore causing leakage. Membrane actions cause tearing if the angle of wrapping is less than 45 deg ($\alpha < 45$ deg) as illustrated

---

[1] Clodfelter, G. A., Development of the Filament-Wound Composite Launch Tubes for the SMAWT Program, US Army Missile Command, Redstone Arsenal, Alabama, March 1975, Technical Report RL-75-8.

in Figure 1. Internal pressure causes a circumferential extension [line AC of Figure 1(a) stretches to line A'C' of Figure 1(b)] and axial contraction (line BD contracts to B'D'); the parallelogram ABCD must dilate to the parallelogram A'B'C'D. The initial fracture of the resin and/or debonding is accompanied by opening and leakage.

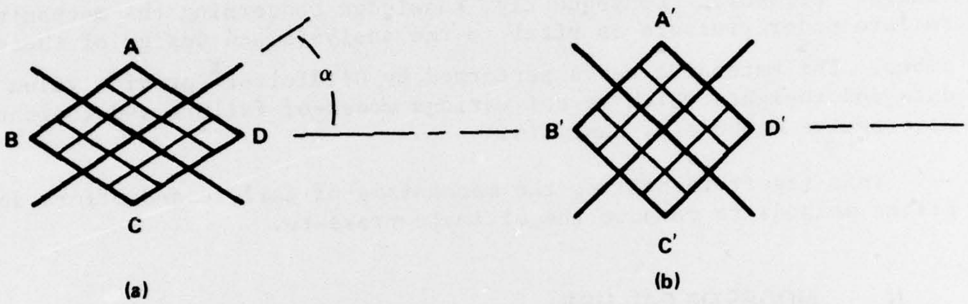

Figure 1. Dilatory actions which initiate failure in tubes with wrap angles less than 45 deg.

The pressure distribution in the tube is shown in Figure 2. It is particularly significant that a narrow region at the ends is not subject to pressure; consequently, the tube bulges as indicated by the dotted lines. This bending causes some extension of the outer axial lines. As the angle of wrapping increases, the axial stiffness decreases and the bending increases; eventually, fracture of the resin and/or debonding produces tearing.*

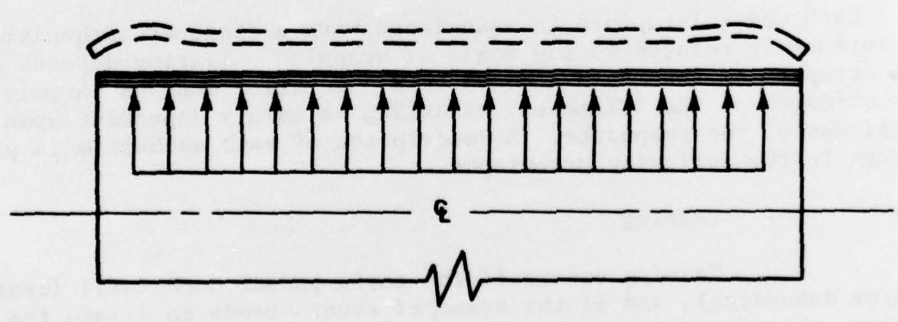

Figure 2. End bulges which initiate failure in tubes with large wrap angles.

***In a previous report, this mode-of-failure was identified as "bursting;" however, because it stems from a failure of the resin and bond, it is now classified as "tearing."**

In summary, tearing is caused by membrane action with small angles (approximately $\alpha < 45$ deg) and by bending action with large angles (approximately $\alpha > 75$ deg), as indicated in Figure 3.

B. Bursting

In a well-designed tube, the high tensile strength of the filaments is realized, and failure occurs via abrupt bursting when the tensile stresses upon the filaments reach their ultimate value. If the angle of wrapping exceeds 45 deg, the netting of filaments contains and compresses the resin by the action shown in Figure 1. Although the resin may fracture, it appears to sustain high shear stresses in this compressed state. If the angle of wrapping is excessive ($\alpha > 75$ deg), the local bending shown in Figure 2 counteracts the membrane action of the netting and causes tearing.

C. Buckling

Experiments have indicated that tubes fail by buckling in the manner of a column. The plot shown in Figure 4 has all the features of the corresponding plot for a column under axial compression. If the tube behaves according to the Euler-Bernoulli theory, the critical pressure is given by the formula:

$$P_c = K \frac{\pi EI}{r^2 l^2} ,$$

where

E = axial modulus

I = moment of inertia of the cross section

l = length between the end supports (O-rings)

r = internal radius

K = a dimensionless factor which depends upon the end supports.

III. ANALYSES OF STRESS, STRAIN, AND ELASTIC BEHAVIOR

In Figure 5, x_1 denotes the length along a filament, x_2 denotes the length along the orthogonal line on the cylinder, X_1 and X_2 denote lengths along the circumferential and axial lines, and $x_3 \equiv X_3$ denotes the radial distance.

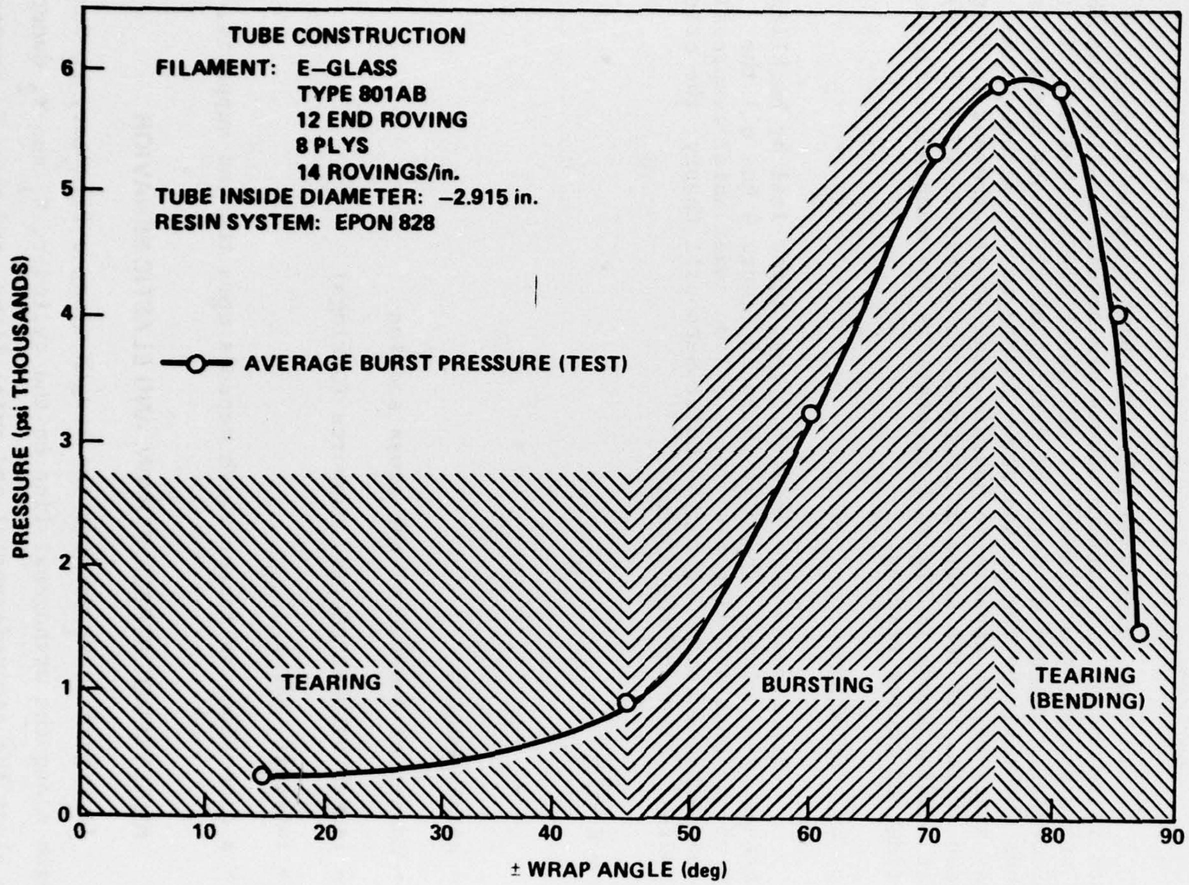

Figure 3. Modes of failure for tubes of various wrap angles.

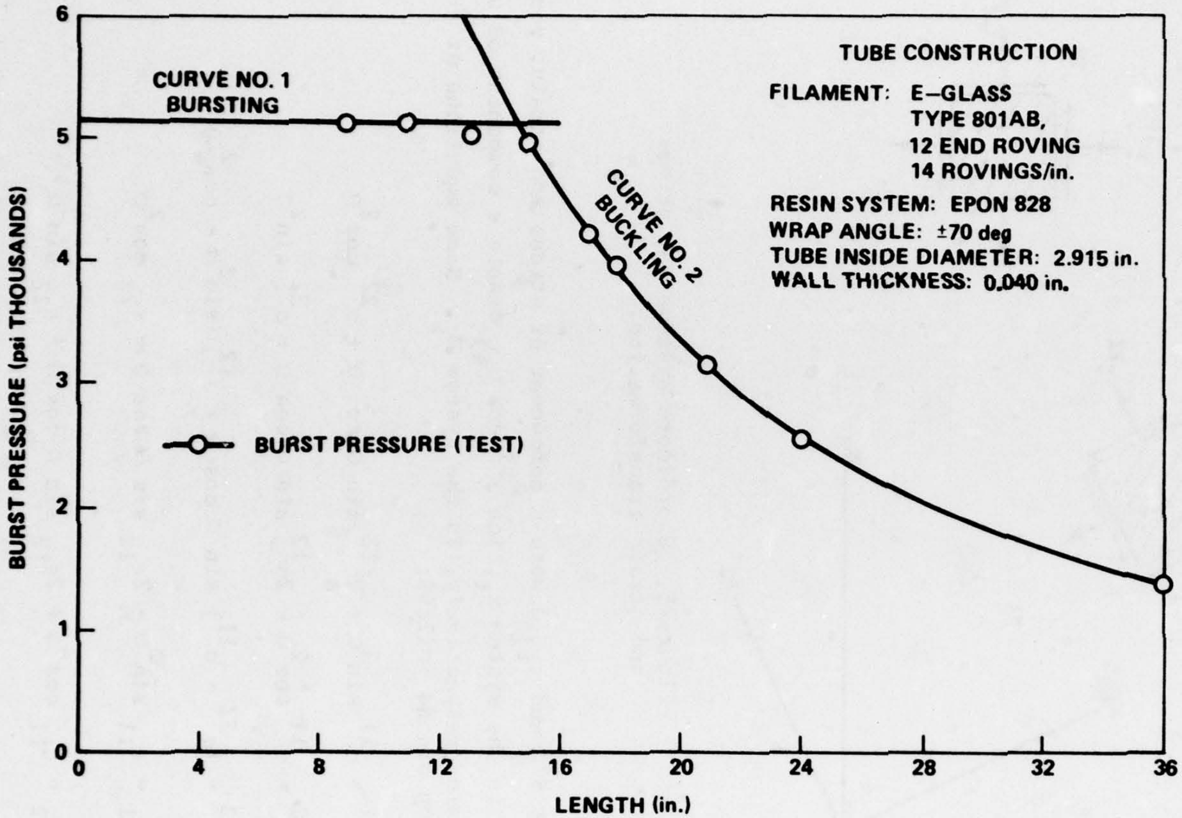

Figure 4. Effect of tube length on ultimate burst pressure.

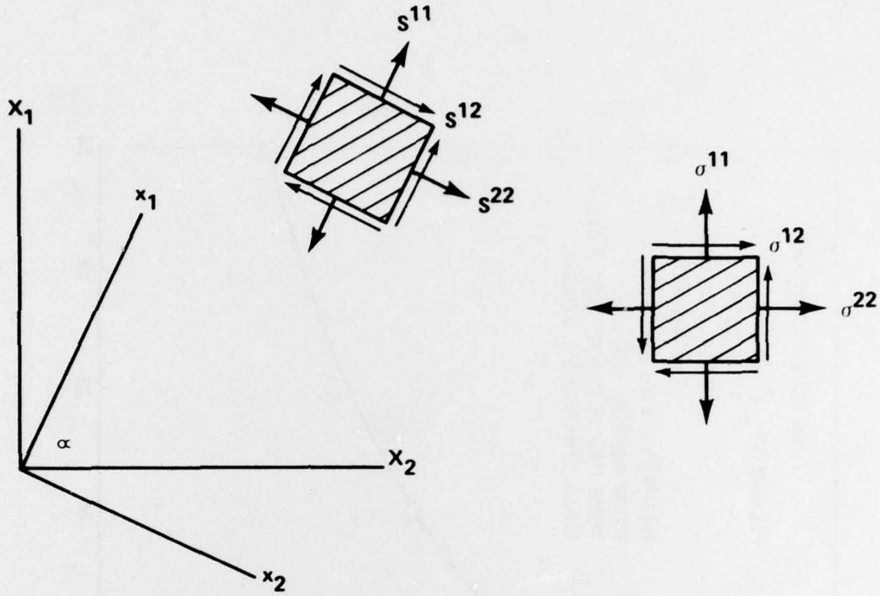

Figure 5. Coordinate systems for stress and strain transformation.

Let S^{ij} and ϵ_{ij} denote a component of stress and strain, respectively, in the system x_i; let σ^{ij} and γ_{ij} denote a component of stress and strain, respectively, in the system X_i. Some equations of transformation are as follows:

$$S^{11} = \sigma^{11} \sin^2\alpha + 2\sigma^{12} \sin\alpha \cos\alpha + \sigma^{22} \cos^2\alpha \tag{2a}$$

$$S^{22} = \sigma^{11} \cos^2\alpha - 2\sigma^{12} \sin\alpha \cos\alpha + \sigma^{22} \sin^2\alpha \tag{2b}$$

$$S^{12} = (\sigma^{22} - \sigma^{11}) \sin\alpha \cos\alpha + \sigma^{12} (\sin^2\alpha - \cos^2\alpha) \tag{2c}$$

$$\gamma_{11} = \epsilon_{11} \sin^2\alpha - 2\epsilon_{12} \sin\alpha \cos\alpha + \epsilon_{22} \cos^2\alpha \tag{3a}$$

$$\gamma_{22} = \epsilon_{11} \cos^2\alpha + 2\epsilon_{12} \sin\alpha \cos\alpha + \epsilon_{22} \sin^2\alpha \tag{3b}$$

$$\gamma_{12} = -(\epsilon_{22} - \epsilon_{11}) \sin\alpha \cos\alpha + \epsilon_{12} (\sin^2 - \cos^2\alpha) \quad . \tag{3c}$$

In Equations (2) and (3), all components are tensorial.

If the constituents behave as Hookean materials,

$$\epsilon^{ij} = C^{ijkl} S_{kl} \quad , \tag{4}$$

where the repeated index implies summation. Estimates of the coefficients (C^{ijkl}) can be calculated from the elastic constants of the glass (filaments) and epoxy (resin). For this purpose, let

E_g, E_r = modulus of elasticity of the glass, resin

ν_g, ν_r = Poisson ratio of the glass, resin

R_g, R_r = part by volume of glass, resin.

Estimates of the upper bounds for the coefficients are based on the assumption that filaments are regularly distributed. The formulas are as follows:

$$C^{1111} = (E_g R_g + E_r R_r)^{-1} \tag{5a}$$

$$C^{1122} = -(\nu_g R_g + \nu_r R_r) C^{1111} \tag{5b}$$

$$C^{2222} = R_g R_r \left[\frac{E_g}{E_r} \left(1 - \nu_r^2\right) + \frac{E_r}{E_g} \left(1 = \nu_g^2\right) + R_g + R_r + 2\nu_r \nu_g \right] C^{1111} \tag{5c}$$

$$C^{1212} = \frac{1}{2} \left[\frac{R_r}{E_r} (1 + \nu_r) + \frac{R_g}{E_g} (1 + \nu_g) \right] \quad . \tag{5d}$$

The moduli of the composite in the circumferential and axial directions follow from Equations (2), (3), and (4):

$$E_1 = \left[C^{1111} \sin^4\alpha + 2(C^{1122} + 2C^{1212}) \sin^2\alpha \cos^2\alpha + C^{2222} \cos^4\alpha \right]^{-1} \tag{6a}$$

$$E_2 = \left[C^{1111} \cos^4\alpha + 2(C^{1122} + 2C^{1212}) \sin^2\alpha \cos^2\alpha + C^{2222} \sin^4\alpha \right]^{-1} \quad . \tag{6b}$$

The coefficients C^{1122} and C^{1212} of Equation (5b) and (5d) are estimates based upon a regular distribution of the filaments. Lower values result if the filaments lie contiguously in layers. The actual values must be determined experimentally. Experiments and computations for the tube shown in Figures 4 and 6 provide the values $E_2 = 1.839 \times 10^6$ and 1.403×10^6 psi, but the latter is understandably lower. Therefore, the calculated coefficients, C^{1122} and C^{1212}, must be similarly reduced to account for the microstructure of the composite.

If the constituents behave as Hookean materials, estimates of the stresses acting upon the resin are as follows:

$$S_r^{11} = \left[E_r S^{11} + R_g(E_g \nu_r = E_r \nu_g)\ S^{22}\right] C^{1111} \tag{7a}$$

$$S_r^{22} = S^{22} \tag{7b}$$

$$S_r^{12} = S^{12} \quad . \tag{7c}$$

A. Tearing

The experimental evidence indicates that the behavior is nearly linear and elastic to the occurrence of tearing, i.e., to the fracture of the resin and/or debonding. If the hoop stress predominates,

$$\sigma^{11} = \frac{pd}{2t} \quad , \quad \sigma^{22} = \sigma^{12} = 0 \quad ,$$

then, according to Equations (2) and (7),

$$S_r^{11} = \frac{pd}{2t}\left[E_r \sin^2\alpha + R_g\ (E_g \nu_r - E_r \nu_g)\ \cos^2\alpha\right] C^{1111} \tag{8a}$$

$$S_r^{22} = \frac{pd}{2t} \cos^2\alpha \tag{8b}$$

$$S_r^{12} = -\frac{pd}{2t} \sin\alpha \cos\alpha \quad . \tag{8c}$$

In this circumstance, the stress components in the resin are linearly related to the pressure by Equation (8), or simply

$$S_r^{11} = C^{11}p \quad , \quad S_r^{22} = C^{22}p \quad , \quad S_r^{12} = C^{12}p \quad ,$$

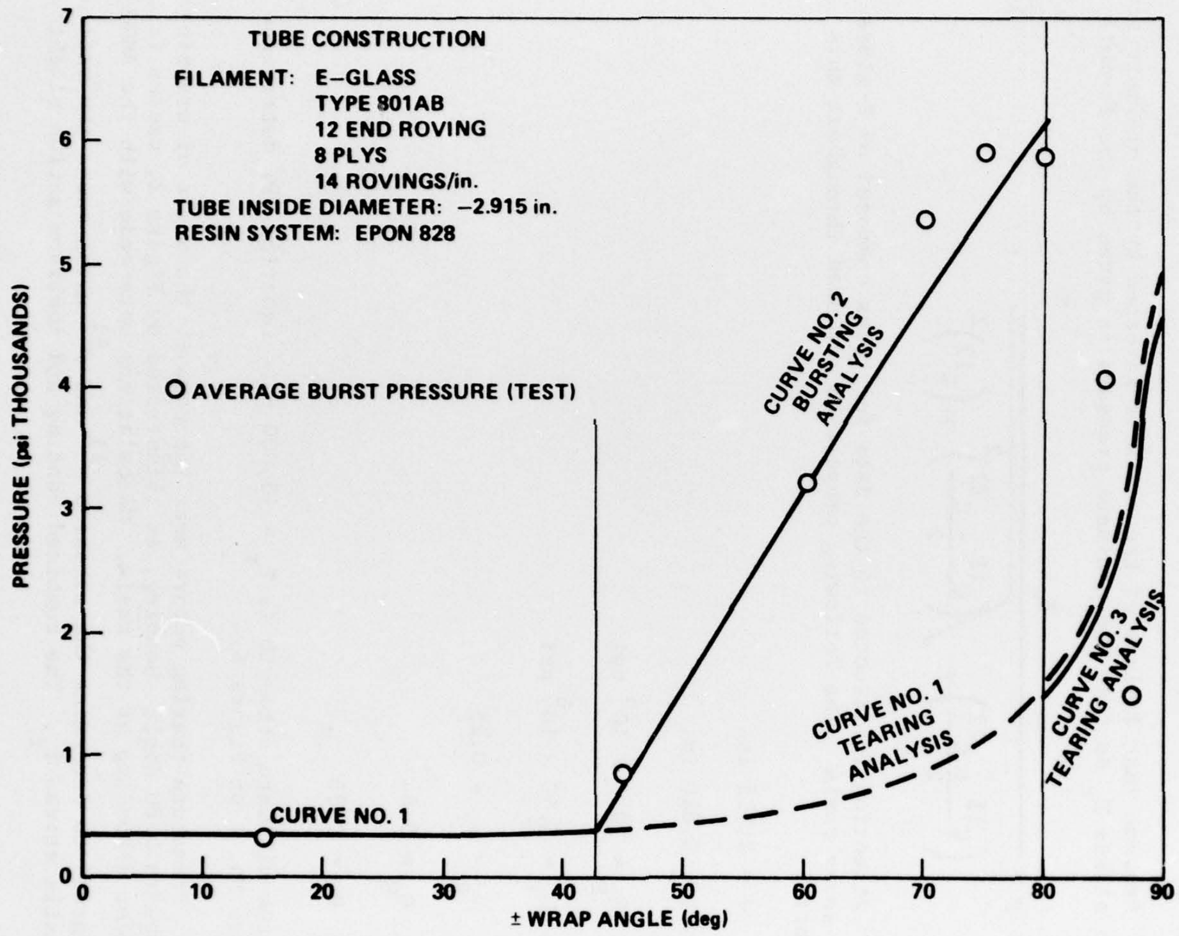

NOTE: TUBE SUBJECTED ONLY TO INTERNAL PRESSURE

Figure 6. Failure predictions by tearing and bursting analysis.

where the coefficients (C^{11}, C^{22}, C^{12}) are determined by the dimensions (d, t), the elastic constants (E_g, E_r, ν_g, ν_r), the ratios of constituents (R_g, R_r), and the angle (α).

Presume that failure of the resin is governed by the ultimate tensile stress T_r so that the ultimate pressure is given by the formula

$$p = \frac{T_r}{\left(\frac{C^{11} + C^{22}}{2}\right) + \sqrt{\left(\frac{C^{11} - C^{22}}{2}\right)^2 + \left(C^{12}\right)^2}} \qquad (9)$$

Attention is directed to the data for tubes composed of E-glass and epoxy resin. The following properties are used throughout this report:

$d = 2.915$ in.

$t = 0.040$ in.

$E_g = 10.5 \times 10^6$ psi

$E_r = 0.50 \times 10^6$ psi

$\nu_g = \nu_r = 0.25$

$R_g = 0.64$

$$R_r = 0.36 \quad . \qquad (10)$$

If the ultimate strength is $T_r = 13{,}000$ psi, Equation (9) determines curve No. 1 of Figure 6.

Premature tearing occurs near the ends if the angle of wrapping is large ($\alpha > 80$ deg). Bending, as illustrated by Figure 2, causes fracture and/or debonding of the resin. Calculations were made with the AMGO program* to determine the stresses σ^{11} and σ^{22} which cause the maximum tensile stress T_r. The combined bending and membrane action slightly

*Program written by J. Brisbane, Rohm and Haas Co., modified and executed by G. Patrick.

reduces the ultimate pressure as indicated by curve No. 3 of Figure 6. Of course, this analysis does not account for end effects which may alter the distributions of stress between the constituents, nor does this analysis provide for imperfections; i.e., cross-overs of the windings that may be particularly significant at the large angles of wrapping.

B. Bursting

This analysis supports the experimental observations of bursting at stresses which exceed the level of initial crazing and debonding. Accordingly, elastic behavior is not presumed, but computations are based on two specific assumptions. If the hydrostatic stress (or mean normal stress) in the resin is compressive, (1) the resin can sustain shear stresses which exceed the level of fracture, and (2) the glass filaments can attain the ultimate tensile stress of the roving (371,000 psi in the present case). The maximum shear stress upon the resin is assumed constant (40,000 psi in the present case).

Figure 7(a) shows an element of the composite wherein the hoop stress σ^{11} is shown decomposed into the normal component of the tensile stress (T_g) upon the filaments and the normal stress (σ_r^{11}) upon the resin:

$$\sigma^{11} = \frac{pd}{2t} = T_g R_g \sin \alpha + \sigma_r^{11} R_r \quad . \tag{11a}$$

Likewise, the vanishing stress (σ^{22}) upon a cross-section is decomposed so that,

$$\sigma^{22} = 0 = T_g R_g \cos \alpha + \sigma_r^{22} R_r \quad . \tag{11b}$$

An element of the resin is shown in Figure 7(b). The condition for equilibrium of components in the direction x_i is as follows:

$$S_r^{12} = \left(\sigma_r^{22} - \sigma_r^{11}\right) \sin \alpha \cos \alpha \quad . \tag{12}$$

From Equation (11), the normal stresses in the resin follow:

$$\sigma_r^{11} = p\left(\frac{d}{2tR_r}\right) - T_g\left(\frac{R_g}{R_r} \sin \alpha\right) \tag{13a}$$

$$\sigma_r^{22} = -T_g\left(\frac{R_g}{R_r} \cos \alpha\right) \quad . \tag{13b}$$

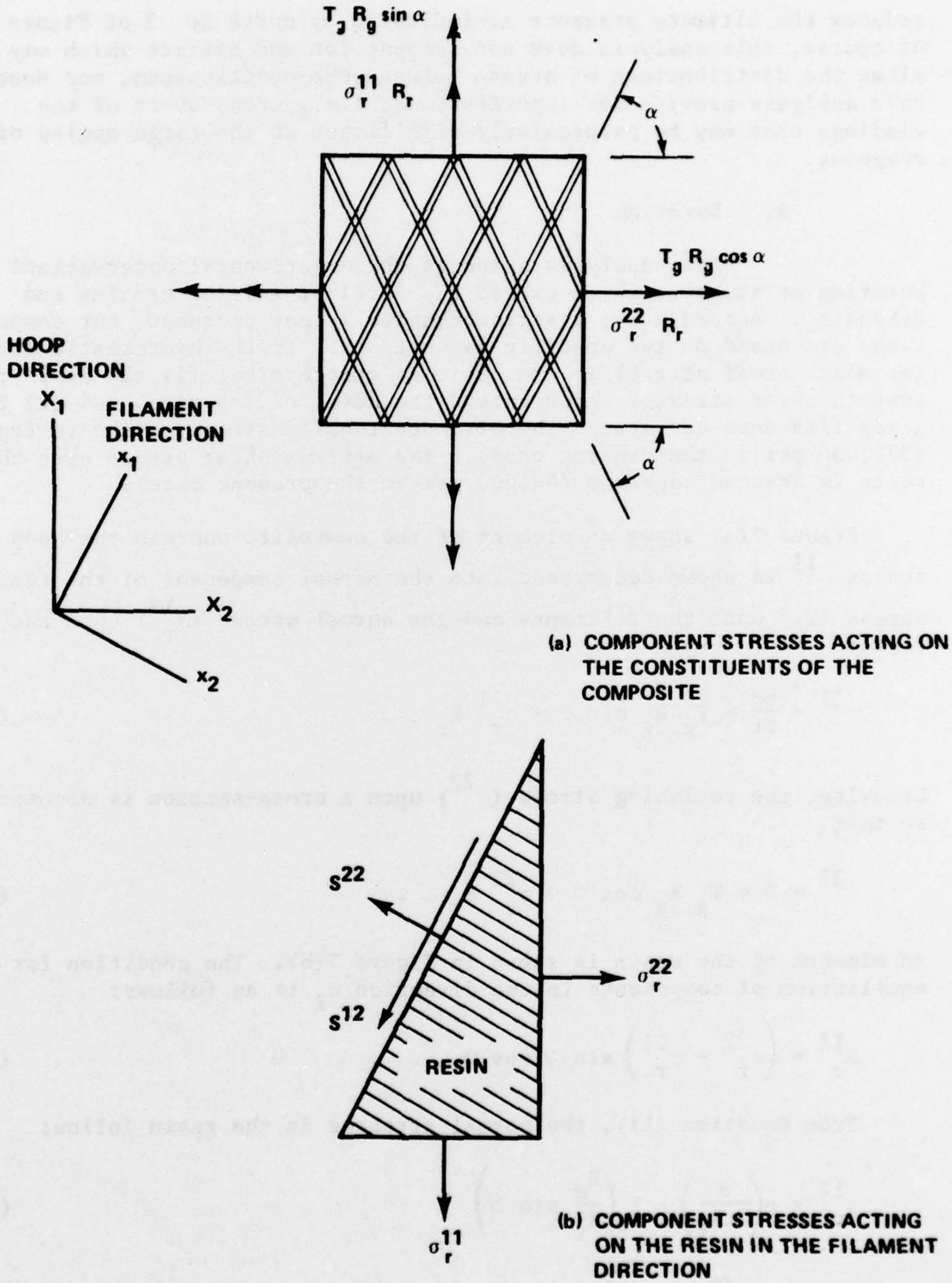

Figure 7. Elements used in bursting analysis.

In accordance with Equation (12), the maximum shear stress in the resin follows:

$$\tau_r = \frac{1}{2}\left(\sigma_r^{11} - \sigma_r^{22}\right) \quad . \tag{13c}$$

For given properties (T_g, τ_r, R_g, R_r) and dimensions (α, d, t), the normal stresses, σ_r^{11} and σ_r^{22}, are given by Equation (13b) and (13c), and the ultimate pressure p is then given by Equation (13a). The computation determines curve No. 2 of Figure 6.

The bursting strengths of curve No. 2 are attained only if the resin can sustain the maximum shear stress (40,000 psi). Even a fractured matrix may sustain the shear stress, provided that the compressive stress is sufficiently great. This calculation indicates that the mean compressive stress diminishes abruptly (from 80,700 to 40,400 psi) as the angle of wrapping increases (from 75 to 82 deg). Consequently, it appears that the angle ($\alpha \doteq 75$ deg) of wrapping imposes a limitation on the validity of the foregoing analysis.

C. Buckling

Experimental observations indicate that the tube may buckle as a column, and suggest that Equation (1) may apply; however, if the factors E and K are constant, then curve No. 1 does not fit the experimental data. If the critical stress should exceed the proportional limit, then the factor E would be the variable modulus; however, the experimental results indicate that the behavior is nearly linear to the buckling pressures of Figure 4 ($\ell > 15$). The factor K is variable if the end conditions are altered. Therefore, one is led to an examination of the end conditions.

The ends of the tubes are pressed over two O-rings contained in a plug. Initially, the clearance between the plug and tube is approximately 0.005 in., and the radial compression of the ring is approximately 0.030 in. At the pressure of 5000 psi, the expansion of the tube ($\gamma_{11} \doteq 0.030$) relieves the compression of the innermost ring and the clearance reaches approximately 0.049 in. At the lower pressure of 1350 psi, the ring remains compressed and the clearance is approximately 0.017 in. Therefore, it appears that the rings provide little more than simple support (K = 1) at the higher pressures (short tubes), but more support ($1 < K < 4$) at the lower pressures (long tubes). For simplicity, assume that the factor K is a linear function of the pressure p; for the tube of Figure 4,

$$K = 1 + 0.76\left(1 - \frac{p}{4300}\right) \quad . \tag{14}$$

Equation (14) implies the simply supported ends (K = 1) at the higher pressure (p = 4300 psi) and elastically-supported ends at the lower pressures (e.g., K = 1.5 at p = 1400 psi). Equations (1) and (14) provide curve No. 1 of Figure 4. The short tubes fail by bursting which is independent of the length as indicated by curve No. 2.

IV. SUMMARY AND RECOMMENDATIONS

The preceding experiments and analyses have served to identify distinct mechanisms of failure (tearing, bursting, and buckling). Moreover, the analyses predict, with reasonable accuracy, the failures of the cylinders under internal pressure; only those cases of large angles of wrapping ($\alpha > 75$ deg) are unpredictable. The latter could be significantly influenced by end conditions and imperfections.

Additional experimentation is needed to obtain enough data to establish a general criterion of failure. The cylindrical tube appears to be well-suited to such experimentation for two reasons: (a) it provides a central portion which has the necessary continuity of constituents, i.e., a portion unaffected by end effects; and (b) the cylindrical tube is an important form of application.

The necessary experimental program should include the following tests:

a) Internal pressure.

b) Axial tension.

c) Axial compression.

d) Torsion.

e) Combinations of axial loads and internal pressure.

In addition to further studies of the composite, more tests are needed to ascertain the properties of the individual constituents (the glass filaments and resins) and the mechanism of adherence and debonding.

In view of the proven qualities (strength and lightness) of those composite tubes, an intensive program of research seems fully warranted.

DISTRIBUTION

	No. of Copies
Defense Documentation Center Cameron Station Alexandria, Virginia 22314	12
Commander US Army Materiel Development and Readiness Command	
ATTN: DRCRD	1
DRCDL	1
5001 Eisenhower Avenue Alexandria, Virginia 22333	
DRSMI-FR, Mr. Strickland	1
-LP, Mr. Voigt	1
-R, Dr. McDaniel	1
Dr. Kobler	1
-RBD	3
-RPR (Record Set)	1
(Reference Copy)	1